ISSN 0915-633X

NATIONAL INSTITUTE FOR FUSION SCIENCE

Various Neutrino Beams Generated by D_2 Gas Discharge

J. Uramoto

(Received - Feb. 10, 1998)

NIFS-545 Mar. 1998

RESEARCH REPORT
NIFS Series

NAGOYA, JAPAN

Various neutrino beams generated by D_2 gas discharge

Jōshin URAMOTO

National Institute for Fusion Science,

Oroshi-cho, Toki-shi, Gifu, 509-5292, Japan

Abstract

From outside of a D_2 gas discharge in magnetic field, positive K mesonlike particles K^+ are extracted with D^+, D_3^+ ions in a low voltage (800V) and are shot into a thick metal plates MP. When positive ions (above a critical ion energy) are supplied in the opposite side of MP, negative muonlike particles μ^-, negative K mesonlike particles K^- and negative τ-like particles τ^- appear continuously while the energies are corresponding to the extraction voltage (800V). From the total thickness of MP, the unknown particles penetrating MP are estimated to be μ-neutrino ν_μ, (K-neutrino ν_k) and τ-neutrino ν_τ. If electrons (above a critical electron energy are supplied in the opposite side of MP, positive muonlike particles μ^+, positive K mesonlike particles K^+ and positive τ-like particles τ^+ appear. Then, the unknown particles are estimated to be anti-μ-neutrino $\bar{\nu}_\mu$, (anti-K-neutrino $\bar{\nu}_k$) and anti-τ-neutrino $\bar{\nu}_\mu$.

Keywords: μ-neutrino ν_μ, (K- neutrino ν_k), τ-neutrino ν_τ

We have reported[1),2)] already that the μ-neutrino ν_μ beam and anti-μ-neutrino $\bar{\nu}_\mu$ beam are produced from a H_2 gas discharge along magnetic field. The origin of ν_μ and $\bar{\nu}_\mu$ beam generation is due to the H^- ion production outside of the H_2 gas discharge. Thus, we can consider naturally that some neutrino beams will be produced also from a D_2 gas discharge along magnetic field as D^- ions are extracted[3)] from outside of the D_2 gas discharge.

Schematic diagrams of the experimental apparatus for a D_2 gas discharge and a mass analyzer are shown in Figs. 1. In the first experiment, D^+, $D_3{}^+$ ions and positive K mesonlike particles K^+ are detected. The positively charged particles extracted from outside of the D_2 gas discharge plasma as shown in Fig 1a, are injected into the ordinary magnetic mass analyzer (MA) through the slit (3 mm × 1 cm) while each mass of the positively charged particle is estimated by the following relations: From the analyzing magnetic field B_M where the positive current to the beam collector BC shows a peak, the curvature radius r of the mass analyzer and the extraction (acceleration) voltage V_E, we can estimate the mass m of the negatively charged particle by,

$$m = \frac{Ze\,(B_M r)^2}{2V_E}$$

$$= \frac{8.8 \times 10^{-2}\, Z\,(B_M r)^2\, m_e}{V_E}, \quad \text{.......} \quad (1)$$

where e is the electron charge, B_M is in gauss unit, r is in cm unit, V_E is in volt unit and m_e is the electron mass and Z is the charge number. For the curvature radius $r = 4.3$ cm of this mass analyzer, the Eq. (1) is rewritten by

$$m = \frac{1.63\, Z\, B_M{}^2}{V_E}\, m_e. \quad \text{.......} \quad (2)$$

In the extraction of positively charged particles, a potential V_L of the first extraction electrode (L) is –6V with respect to the discharge anode, a potential V_M of the second extraction electrode (M) is –300V and a potential V_E of the final extraction electrode (E) in –800V.

The dependences of the positive current I^+ to BC on B_M are shown in Fig. 2. Obviously, in Fig. 2, a large peak of I^+ at $B_M \approx (5.5 \times 240)$ gauss = 1320 gauss is corresponding to D^+ ion, assuming that Z = 1 in Eq. (2). That is, we obtain m ≈ 3700 m_e as $|V_E|$ = 800V. (Another large peak of I^+ is observed at $B_M \approx 2300$ gauss, which is corresponding to D_3^+).

Next, a main small peak of I^+ to BC is seen in Fig. 2. We find that the main small peak at $B_M \approx (2.7 \times 240)$ gauss ≈ 665 gauss is corresponding to a positive K mesonlike (K^+) particle, assuming that $Z = 1$ in Eq. (2). That is, we obtain $m \approx 900\ m_e$ (near the true K meson mass $966\ m_e$) for the main small peak.

The second experimental apparatus is shown in Fig. 3. There, some positive ions are supplied externally by a positive ion gun (I.G.) using electron beam reflections in residual gases inside the vacuum chamber. Then, the mass analyzer and the ion gun are composed as an independent detector for unknown particles which penetrate thick metal plates (totally, above 10 cm) and atmosphere without energy loss. In Fig. 3 a, the unknown particle "source" is constructed from extraction electrodes L, M with multi apertures ($3\phi \times 100$ apertures in 40 cm^2 area) and a thick metal plate E. Thus, the unknown particles can enter the slit of MA easily even if a distance between the unknown particle "source" and the "detector" is very long (~ 50 cm at present). The unknown particles induced by the positive K meson K^+ particles, enter the "detector" after a flight of about 50 cm through the metal plates and atmosphere. In the detector side, a (negative muonlike particle) μ^- beam, a (negative K mesonlike particle) K^- beam and a (negative τ like particle) τ^- beam are observed at the beam collector BC of MA when the positive ion beam is supplied behind the detector side metal plate DMP as shown in Fig. 3 b. The positive ion beam is produced from the residual gas (air) ionization (~ 10^{-5} Torr) by the electron beam reflections. The positive ion density behind DMP is about 0.3 $\mu A/cm^2$ for an electron acceleration voltage $V_e \approx 350V$ and an electron current of 10 mA to the electron gun anode. Dependences of the negative current I^- on the analyzing magnetic field B_M are shown in Fig. 3 c. From the experimental results, the detected particles are determined to be negative muonlike particle, negative K mesonlike particles and negative τ like particles from Eq. (2) and the particle energies are determined by the extraction voltage V_E in the source side.

If the positive ion beam is not supplied behind DMP, no current to BC of MA appear. That is, the positive ion beam supply is a necessary condition to observe the μ^-, K^- and τ^- beam in the detector side. We find a lower limit of the supplied ion beam energy varying the initial electron beam acceleration voltage V_e. The lower limit energy is about 200 eV for the extraction voltage of

K^+ in the source $|V_E| = 800V$. A relation between V_e and V_E is determined: That is, $V_e > |V_E/4|$ is a necessary condition to observe the μ^-, K^- and τ^- in the detector side.

From the investigations[1),2)] for the H_2 gas discharge, we can consider that the unknown particles penetrating the thick metal plates and passing the atmosphere, are various neutrinos. Furthermore, we can consider the following processes: the μ^- in the detector side is due to ν_μ neutrino beams generated secondarily by some fundamental particles in the D_2 gas discharge source and the τ^- is due to ν_τ neutrino beams. However, the K^- is not explained as "K neutrino ν_k" has not been found up to now.

In this experimental research, negative K mesonlike particles K^- are extracted also with D^- ions from the outside of the D_2 gas discharge as shown in Fig. 1 a and are shot into thick metal plates MP. As the results in the <Detector side> as shown in Fig. 3b, the μ^-, K^- and τ^- appear if the positive ions are supplied, and the μ^+, K^+ and τ^+ appear if the electrons are supplied as shown in Fig. 4b. That is, the characteristics do not depend on the initial extractions of (D^+ and K^+) or (D^- and K^-). Thus, the (ν_μ, ν_k and ν_τ) and the anti-neutrinos ($\bar{\nu}_\mu$, $\bar{\nu}_k$ and $\bar{\nu}_\tau$) co-exist also as seen for the H_2 gas discharge.

References

1) J. Uramoto: Research Report, NIFS–541 (1998).

2) J. Uramoto: Research Report, NIFS–542 (1998).

3) J. Uramoto: National Institute for Fusion Science, Oroshi-cho, Toki-shi, Gifu, 509-5292, Japan – Research Report, NIFS–532 (1998).

Figure Captions

Fig. 1 Schematic diagrams of the experiment apparatus are shown. The apparatus **a** is constructed from a D_2 gas discharge in magnetic fields, three extraction electrodes (with an aperture of 3 mm in diameter) to extract some positively charged particles and a magnetic mass analyzer of 90° deflection type **b**.

a 1: Discharge cathode. 2 and 3: Discharge intermediate electrodes. 4: Discharge power supply. 5: H_2 gas flow. 6: Vacuum pump. 7: Area where cylindrical plasma is transformed into sheet plasma. 8: Insulator. 9: A pair of permanent magnets. 10: Magnetic field coils. 11: Discharge anode. I_A: Discharge anode current. CP: Cylindrical plasma. SP: Sheet plasma. B_Z: Magnetic field. L: First extraction electrode (Potential V_L = –6V). M: Second extraction electrode. E: Final extraction electrode. V_M: Potential (–300V) of second extraction electrode with respect to discharge anode. V_E: Potential (–800V) of final extraction electrode with respect to discharge anode. MA: Magnetic deflection (90°) mass analyzer. B_M: Magnetic field intensity of MA. BC: Beam collector of MA. I^+: Positive current to BC. $D_0{}^+$: Deuteron positive ions outside of sheet plasma. D^+: Accelerated deuteron positive ions. $K_0{}^+$: Positive K mesonlike particles outside of sheet plasma. K^+: Accelerated positive K mesonlike particles.

b S: Entrance slit (3 mm × 10 mm) of MA. Fe: shows Iron. C: Magnetic coil. (N): North pole of electro-magnet. (S): South pole.

In order to extract D^+ ions over wide area, the discharge (cylindrical) plasma flow of about 1 cm in diameter is transformed into a sheet plasma flow of about 3 mm in thickness and about 20 cm in width. The sheet plasma flow enters the anode through the main chamber (50 cm long). A uniform magnetic field of about 50 gauss is applied along the sheet plasma flow in the main chamber where the D_2 gas pressure is about 1.5×10^{-3} Torr. The discharge anode current I_A is 20A and the discharge voltage is 95V. A distance between the sheet plasma center and the first extraction electrode (L) is 7.5 cm. The plasma density in the center of the sheet plasma is about 10^{11}/cc and the electron temperature is about 20 eV. The positive ion density in front of the first extraction electrode is estimated to be about 10^{10}/cc from a positive ion saturation current as $D_3{}^+$, while the electron density from the Langmuir probe characteristic is about 10^9/cc and the electron temperature is about 3.0 eV. That is, the electron density in front of the first extraction electrode is reduced near 1/10 of the positive ion density as D^- ions are produced outside of the D_2 gas discharge plasma.

Fig. 2 A dependence of positive current I^+ to the beam collector BC on the analyzing magnetic field B_M is shown under a final extraction voltage $V_E = -800V$, the second extraction electrode voltage $V_M = -300V$ and the first extraction electrode voltage $V_L = -6V$. D^+ shows current peak corresponding to D^+ ions. K^+ shows a current peak corresponding to a positive K mesonlike particle which is estimated from the mass. μ^+ shows a current peak corresponding to a positive muonlike particle.

Fig. 3 **a** A schematic diagram of the large area ν_μ, (ν_k) and ν_τ beam sources is shown where 100 apertures in an area of 40 cm^2 are opened in the first extraction electrode L and the second extraction electrode M, and where the final extraction electrode E is a thick metal plate (of 3 cm in thickness) without apertures. ν_τ: t neutrino. (ν_k: K neutrino).

b A schematic diagram of the ν_μ, (ν_k) and ν_τ beam detector is shown where DMP is a thick metal plate (3 cm in thickness) which receives the many ν_μ, (ν_k) and ν_τ beams. I.G. is a positive ion gun where a positive ion beam is produced by multi-reflections of the electron beam in residual gases (air, He, Ar are tested). The electron beam is generated by an electron gun with a filament cathode and an anode electrode. V_e is a power supply of the electron gun.

c Dependences of the negative current I^- to BC on the reversed analyzing magnetic field $-B_M$ are shown where three current peaks of I^- are corresponding to μ^-, K^- and τ^- particles.

Fig. 4 **a** A schematic diagram of the large area anti-neutrino $\bar{\nu}_\mu$, $(\bar{\nu}_k)$ and $\bar{\nu}_\tau$ beams. D_0^-: D^- ions outside of D_2 gad discharge. K_0^-: Negative K mesonlike particles outside of D_2 gas discharge.

b A schematic diagram of the anti-neutrino beam detector. E.G.: Electron gun. e^- Beam: Electron beam.

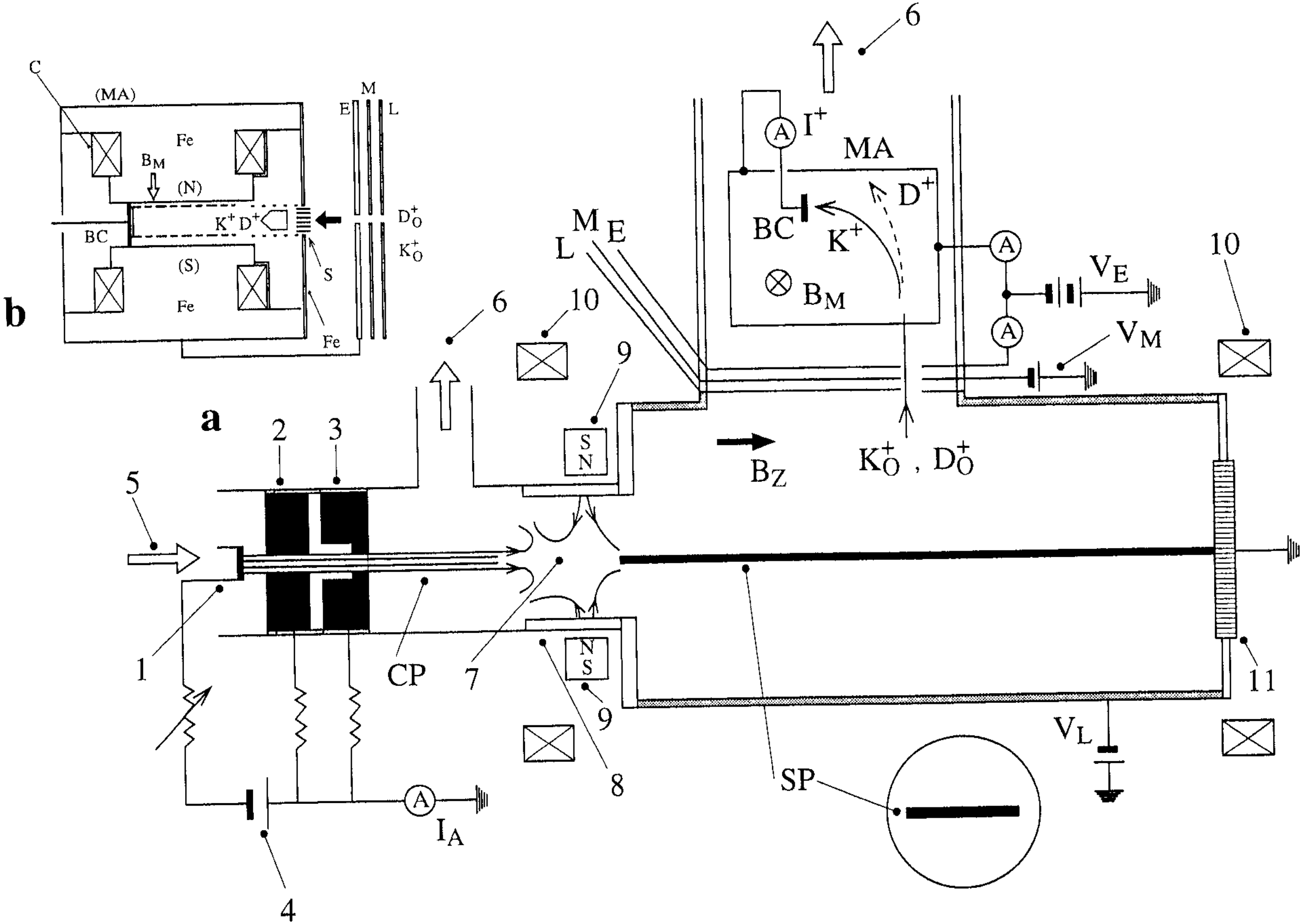

b
C
(MA)
Fe
B_M
(N)
BC
K+ D+
(S)
Fe
S
Fe
E
M
L
D+O
K+O
a
1
2
3
4
5
6
7
8
9
10
11
CP
L
M
E
MA
I+
BC
K+
D+
B_M
V_E
V_M
B_Z
K+O , D+O
V_L
SP
I_A

Fig. 1

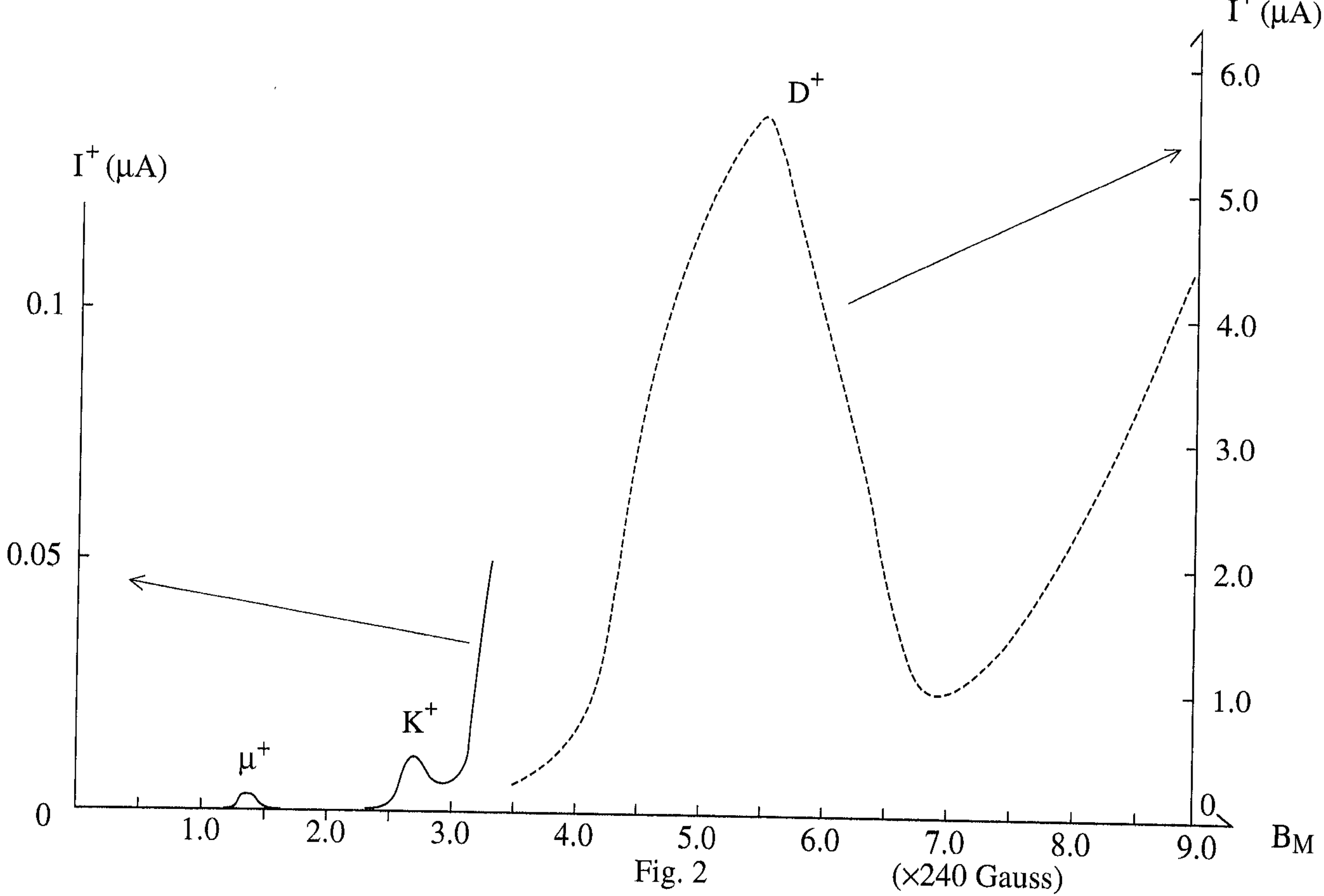

I+ (μA)
0.1
0.05
0
μ+
K+
D+
1.0
2.0
3.0
4.0
5.0
6.0
7.0
8.0
9.0
(×240 Gauss)
B_M
I+ (μA)
6.0
5.0
4.0
3.0
2.0
1.0
0

Fig. 2

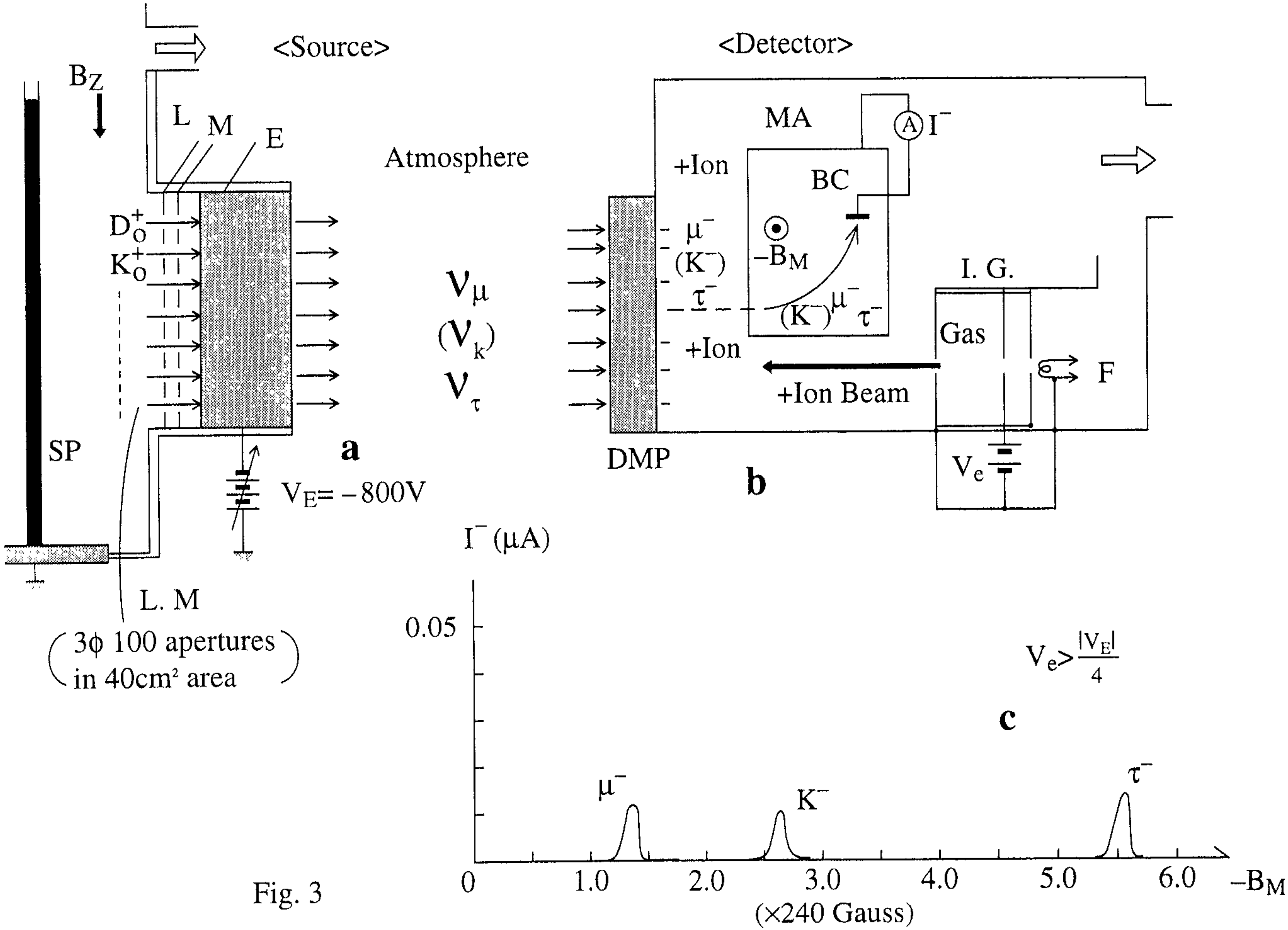

<Source>
<Detector>
B_Z
L
M
E
Atmosphere
D_O^+
K_O^+
SP
a
V_E= −800V
L. M
3ϕ 100 apertures
in 40cm² area
ν_μ
(ν_k)
ν_τ
MA
A I⁻
+Ion
BC
μ⁻
(K⁻)
−B_M
τ⁻
(K⁻) μ⁻ τ⁻
I. G.
Gas
+Ion
F
+Ion Beam
DMP
V_e
b
I⁻ (μA)
0.05
V_e > |V_E|/4
c
μ⁻
K⁻
τ⁻
0
1.0
2.0
3.0
4.0
5.0
6.0
−B_M
(×240 Gauss)

Fig. 3

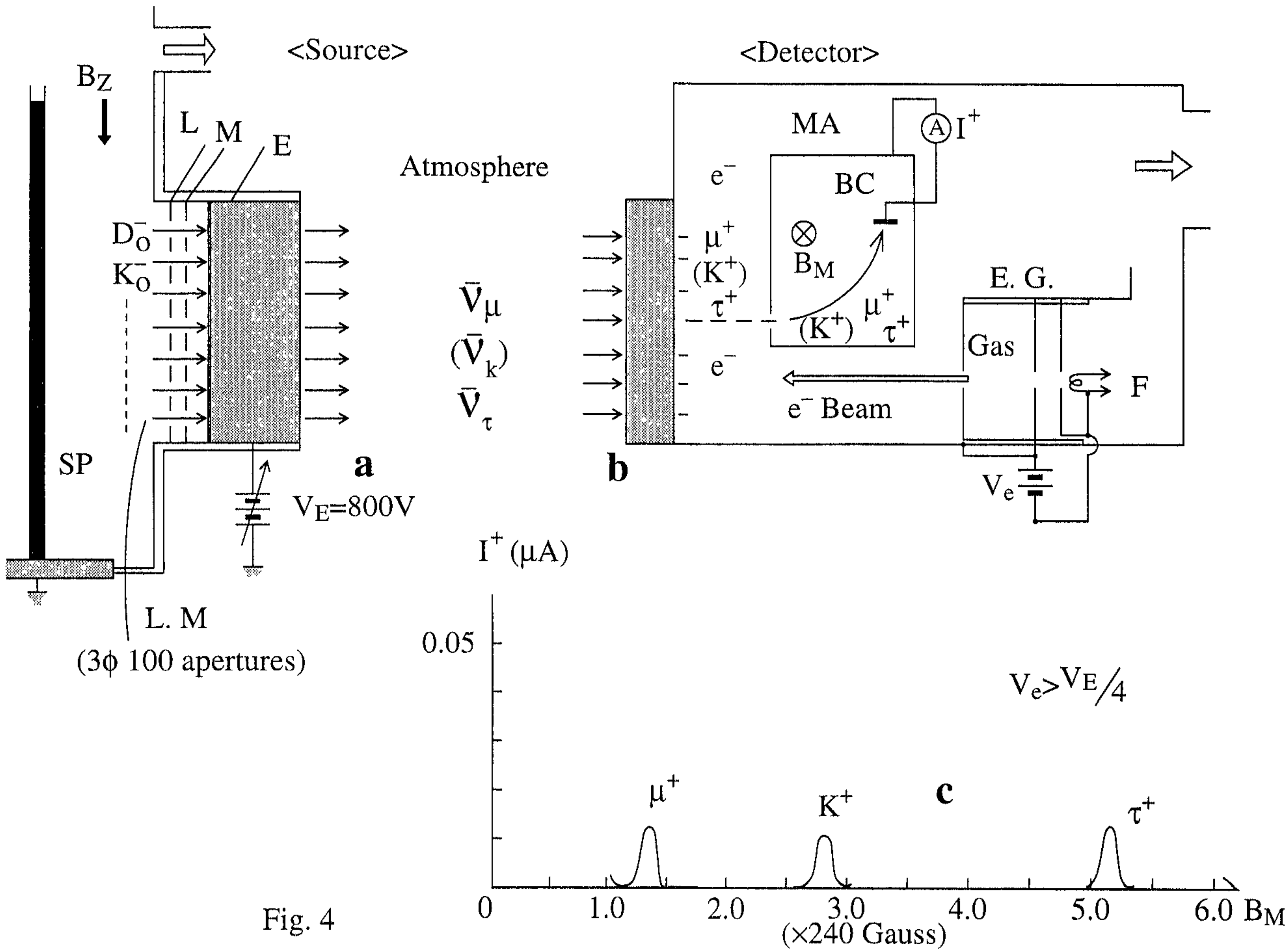

<Source>
<Detector>
B_Z
L
M
E
Atmosphere
D_O^-
K_O^-
SP
a
V_E=800V
L. M
(3φ 100 apertures)
$\bar{\nu}_\mu$
($\bar{\nu}_k$)
$\bar{\nu}_\tau$
MA
A
I^+
e^-
BC
B_M
μ^+
(K^+)
τ^+
E. G.
Gas
F
e^- Beam
b
V_e
I^+ (μA)
0.05
V_e>V_E/4
μ^+
K^+
c
τ^+
0
1.0
2.0
3.0
4.0
5.0
6.0
B_M
(×240 Gauss)

Fig. 4

Recent Issues of NIFS Series

NIFS-510 C.C. Hegna and N. Nakajima,
On the Stability of Mercier and Ballooning Modes in Stellarator Configurations; Oct. 1997

NIFS-511 K. Orito and T. Hatori,
Rotation and Oscillation of Nonlinear Dipole Vortex in the Drift-Unstable Plasma; Oct. 1997

NIFS-512 J. Uramoto,
Clear Detection of Negative Pionlike Particles from H_2 Gas Discharge in Magnetic Field; Oct. 1997

NIFS-513 T. Shimozuma, M. Sato, Y. Takita, S. Ito, S. Kubo, H. Idei, K. Ohkubo, T. Watari, T.S. Chu, K. Felch, P. Cahalan and C.M. Loring, Jr,
The First Preliminary Experiments on an 84 GHz Gyrotron with a Single-Stage Depressed Collector; Oct. 1997

NIFS-514 T. Shjmozuma, S. Morimoto, M. Sato, Y. Takita, S. Ito, S. Kubo, H. Idei, K. Ohkubo and T. Watari,
A Forced Gas-Cooled Single-Disk Window Using Silicon Nitride Composite for High Power CW Millimeter Waves; Oct. 1997

NIFS-515 K. Akaishi,
On the Solution of the Outgassing Equation for the Pump-down of an Unbaked Vacuum System; Oct. 1997

NIFS-516 *Papers Presented at the 6th H-mode Workshop (Seeon, Germany)*; Oct. 1997

NIFS-517 John L. Johnson,
The Quest for Fusion Energy; Oct. 1997

NIFS-518 J. Chen, N. Nakajima and M. Okamoto,
Shift-and-Inverse Lanczos Algorithm for Ideal MHD Stability Analysis; Nov. 1997

NIFS-519 M. Yokoyama, N. Nakajima and M. Okamoto,
Nonlinear Incompressible Poloidal Viscosity in L=2 Heliotron and Quasi-Symmetric Stellarators; Nov. 1997

NIFS-520 S. Kida and H. Miura,
Identificaiton and Analysis of Vortical Structures; Nov. 1997

NIFS-521 K. Ida, S. Nishimura, T. Minami, K. Tanaka, S. Okamura, M. Osakabe, H. Idei, S. Kubo, C. Takahashi and K. Matsuoka,
High Ion Temperature Mode in CHS Heliotron/torsatron Plasmas; Nov. 1997

NIFS-522 M. Yokoyama, N. Nakajima and M. Okamoto,
Realization and Classification of Symmetric Stellarator Configurations through Plasma Boundary Modulations; Dec. 1997

NIFS-523 H. Kitauchi,
Topological Structure of Magnetic Flux Lines Generated by Thermal Convection in a Rotating Spherical Shell; Dec. 1997

NIFS-524 T. Ohkawa,
Tunneling Electron Trap; Dec. 1997

NIFS-525 K. Itoh, S.-I. Itoh, M. Yagi, A. Fukuyama,
Solitary Radial Electric Field Structure in Tokamak Plasmas; Dec. 1997

NIFS-526 Andrey N. Lyakhov,
Alfven Instabilities in FRC Plasma; Dec. 1997

NIFS-527 J. Uramoto,
Net Current Increment of negative Muonlike Particle Produced by the Electron and Posititve Ion Bunch-method; Dec. 1997

NIFS-528 Andrey N. Lyakhov,
Comments on Electrostastic Drift Instabilities in Field Reversed Configuraiton; Dec. 1997

NIFS-529 J. Uramoto,
Pair Creation of Negative and Positive Pionlike (Muonlike) Particle by Interaction between an Electron Bunch and a Positive Ion Bunch; Dec. 1997

NIFS-530 J. Uramoto,
Measuring Method of Decay Time of Negative Muonlike Particle by Beam Collector Applied RF Bias Voltage; Dec. 1997

NIFS-531 J. Uramoto,
Confirmation Method for Metal Plate Penetration of Low Energy Negative Pionlike or Muonlike Particle Beam under Positive Ions; Dec. 1997

NIFS-532 J. Uramoto,
Pair Creations of Negative and Positive Pionlike (Muonlike) Particle or K Mesonlike (Muonlike) Particle in H2 or D2 Gas Discharge in Magnetic Field; Dec. 1997

NIFS-533 S. Kawata, C. Boonmee, T. Teramoto, L. Drska, J. Limpouch, R. Liska, M. Sinor,
Computer-Assisted Particle-in-Cell Code Development; Dec. 1997

NIFS-534 Y. Matsukawa, T. Suda, S. Ohnuki and C. Namba,
Microstructure and Mechanical Property of Neutron Irradiated TiNi Shape Memory Alloy; Jan. 1998

NIFS-535 A. Fujisawa, H. Iguchi, H. Idei, S. Kubo, K. Matsuoka, S. Okamura, K. Tanaka, T. Minami, S. Ohdachi, S. Morita, H. Zushi, S. Lee, M. Osakabe, R. Akiyama, Y. Yoshimura, K. Toi, H. Sanuki, K. Itoh, A. Shimizu, S. Takagi, A. Ejiri, C. Takahashi, M. Kojima, S. Hidekuma, K. Ida, S. Nishimura, N. Inoue, R. Sakamoto, S.-I. Itoh, Y. Hamada, M. Fujiwara,
Discovery of Electric Pulsation in a Toroidal Helical Plasma; Jan. 1998

NIFS-536 Lj.R. Hadzievski, M.M. Skoric, M. Kono and T. Sato,
Simulation of Weak and Strong Langmuir Collapse Regimes; Jan. 1998

NIFS-537 H. Sugama, W. Horton,
Nonlinear Electromagnetic Gyrokinetic Equation for Plasmas with Large Mean Flows; Feb. 1998

NIFS-538 H. Iguchi, T.P. Crowley, A. Fujisawa, S. Lee, K. Tanaka, T. Minami, S. Nishimura, K. Ida, R. Akiyama, Y. Hamada, H., Idei, M. Isobe, M. Kojima, S. Kubo, S. Morita, S. Ohdachi, S. Okamura, M. Osakabe, K. Matsuoka, C. Takahashi and K. Toi,
Space Potential Fluctuations during MHD Activities in the Compact Helical System (CHS); Feb. 1998

NIFS-539 Takashi Yabe and Yan Zhang,
Effect of Ambient Gas on Three-Dimensional Breakup in Coronet Formation Process; Feb. 1998

NIFS-540 H. Nakamura, K. Ikeda and S. Yamaguchi,
Transport Coefficients of InSb in a Strong Magnetic Field; Feb. 1998

NIFS-541 J. Uramoto,
Development of v_μ Beam Detector and Large Area v_μ Beam Source by H_2 Gas Discharge (I); Mar. 1998

NIFS-542 J. Uramoto,
Development of bar{v}$_\mu$ Beam Detector and Large Area bar{v}$_\mu$ Beam Source by H_2 Gas Discharge (II); Mar. 1998

NIFS-543 J. Uramoto,
Some Problems inside a Mass Analyzer for Pions Extracted from a H_2 Gas Discharge; Mar. 1998

NIFS-544 J. Uramoto,
Simplified v_μ, bar{ v}$_\mu$ Beam Detector and v_μ, bar{v}$_\mu$ Beam Source by Interaction between an Electron Bunch and a Positive Ion Bunch; Mar. 1998

NIFS-545 J. Uramoto,
Various Neutrino Beams Generated by D_2 Gas Discharge; Mar.1998

NIFS-546 R. Kanno, N. Nakajima, T. Hayashi and M. Okamoto,
Computational Study of Three Dimensional Equilibria with the Bootstrap Current; Mar. 1998